

Structural investigation of hemicelluloses from *Plantago ovata*, *Mimosa pudica* and *Lallemantia royleana* by MALDI-ToF mass spectrometry

Fozia Iram, Shazma Massey, Mohammad S Iqbal & Douglas G. Ward

To cite this article: Fozia Iram, Shazma Massey, Mohammad S Iqbal & Douglas G. Ward (2018): Structural investigation of hemicelluloses from *Plantago ovata*, *Mimosa pudica* and *Lallemantia royleana* by MALDI-ToF mass spectrometry, Journal of Carbohydrate Chemistry, DOI: 10.1080/07328303.2018.1487973

To link to this article: <https://doi.org/10.1080/07328303.2018.1487973>



Published online: 11 Sep 2018.



Submit your article to this journal [↗](#)






Article views: 8



View Crossmark data [↗](#)



Structural investigation of hemicelluloses from *Plantago ovata*, *Mimosa pudica* and *Lallemantia royleana* by MALDI-ToF mass spectrometry

Fozia Iram^a , Shazma Massey^b, Mohammad S Iqbal^b , and Douglas G. Ward^c 

^aDepartment of Chemistry, LCW University, Lahore, Pakistan; ^bDepartment of Chemistry, Forman Christian College, Lahore, Pakistan; ^cInstitute of Cancer and Genomic Sciences, University of Birmingham, Birmingham, United Kingdom

ABSTRACT

This work concerns structural investigation of water-extractable hemicelluloses from seed husk of *Plantago ovata* and seeds of *Mimosa pudica* and *Lallemantia royleana*. The composition of the materials was determined by CHN elemental analysis, FT-IR spectrometry and monosaccharide analysis. The detailed structural analysis was carried out by MALDI-ToF mass spectrometry. The absence of nitrogen in the materials suggested that they were free from proteins. The isolated materials were found to be branched hemicelluloses. The mass spectrometric study showed presence of β -1,4-linked xylose with arabinose attached to main chain at β -1,3 positions (*Plantago ovata*), β -1,4-linked xylose with glucose attached to main chain at β -1,3 positions (*Mimosa pudica*), and β -1,2-linked rhamnose and β -1,3-linked arabinose units in the main chain with arabinose attached to the main chain through β -1,3-linkage (*Lallemantia royleana*).

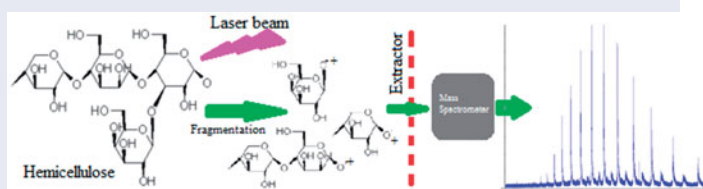
ARTICLE HISTORY

Received 8 February 2018
Accepted 16 May 2018

KEYWORDS

Carbohydrate; hemicellulose; MALDI-ToF; mass spectrometry; polysaccharide; structural analysis

GRAPHICAL ABSTRACT



Introduction

Hemicelluloses are extensively used as functional foods and herbal medicines. They have great potential for use as excipients in pharmaceutical formulations. Currently, cellulose-based materials, such as

carboxymethylcellulose, hydroxypropylcellulose, and hydroxypropyl methylcellulose, are being used commercially as binding, thickening, and suspending agents in various formulations.^[1–5] Cellulosic materials are less biocompatible as compared with hemicelluloses due to the fact that the former are not digestible by humans while the latter are. So, the pharmaceutical excipients developed from hemicelluloses would be more appropriate. Hemicelluloses also possess good water holding capacity and are capable of forming gels. Recently, they gained attention for their use in the formulation of targeted and sustained drug delivery devices^[6–8] and most importantly as scaffolds in tissue engineering.^[9–11] Use of hemicelluloses will be more attractive due to their abundant availability at very low prices. In order to evaluate these materials for such versatile applications, it is desirable to have a comprehensive knowledge of their chemical composition and structural features.

Molar mass of macromolecules plays a significant role in drug delivery.^[12–14] Mass-spectrometric techniques, specifically, electrospray ionization mass spectrometry (ESI-MS) and matrix-assisted laser desorption ionization-time of flight mass spectrometry (MALDI-ToF), are being used for determination of the molar mass of macromolecules. These techniques have been employed in the structural investigation of hemicelluloses. However, most of the hemicelluloses are polydisperse with respect to molecular size, thus the use of ESI-MS has not been considered suitable^[15] as multiple peaks are produced by these materials. This limitation may not be due to polydispersity alone; MALDI may be more appropriate as it produces singly charged ions. Furthermore, ionization efficiency of hemicelluloses is low in ESI due to lower proton affinity of carbohydrates.^[15] Therefore, MALDI-ToF was selected for mass analysis of hemicelluloses in the present work. However, analysis of non-derivatized hemicelluloses by this technique is a challenge due to the off-hand availability of suitable matrices.^[16] For this purpose, derivatization has been considered^[17] but derivatization alters structural features of the materials. Moreover, efficiencies of derivatization of polysaccharides usually vary. Thus, analysis of non-derivatized hemicelluloses by MALDI becomes a challenge.

The objective of this study was to determine structural features of underivatized water-extractable fractions of hemicelluloses from *Plantago ovata* (PO), *Mimosa pudica* (MP), and *Lallemantia royleana* (LR), mainly by MALDI-ToF analysis. All of these materials are from renewable sources and abundantly available in most parts of the world. They form mucilages in water. A detailed thermal analysis of these materials has previously been reported by our group,^[8,18] which suggests that they possess good thermal stabilities for use in pharmaceuticals. These materials are benign to immune system, thus have no toxicity issue.^[6,19,20]

In order to produce meaningful mass spectral signals, various matrices have been investigated.^[21–26] After a preliminary work with 3-amino-4-hydroxybenzoic acid and 2,5-dihydroxybenzoic acid, it was discovered that the latter afforded better reproducibility and higher signal-to-noise ratio.^[24] Since then, it has become the first choice matrix for oligosaccharides. To the best of our knowledge, there have been no reports on MALDI-ToF measurements of un-derivatized hemicelluloses having a molar mass higher than 10,000 Da.^[27,28] In the present work, various analytical techniques have been used along with MALDI-ToF mass spectrometry to carry out a structural investigation of the materials under investigation. The hypothesis of the research was: MALDI-ToF mass spectrometry would provide useful structural information of non-derivatized hemicelluloses.

Results and discussion

The materials extracted by water at room temperature ($25 \pm 2^\circ\text{C}$) from *PO*, *MP*, and *LR* were characterized by CHN elemental analysis, monosaccharide analysis, FT-IR spectroscopy and gel permeation chromatography (GPC). The results of these analyses were found to be similar to those previously reported by our laboratories;^[6] this established the identity of the materials as hemicelluloses. Results of the elemental analysis are given in Table 1. The percentages of C and H of the isolated materials were 29.83–41.98 and 4.63–6.08, respectively, on dry-substance (anhydrous) basis. Nitrogen was below the detection limit. These values are lower than those of other natural polysaccharides ($\sim 45\%$ C and $\sim 6.1\%$ H), which may be due to higher ash content,^[29] i.e. 10–15% in these materials. The absence of N suggests that the materials are free from proteins. The yields were 38, 14, and 12% *w/w* for *PO*, *MP*, and *LR*, respectively.

Results of monosaccharide analysis are given in Table 1. On the basis of monosaccharide contents, the materials were named as arabinoxylan (*AX*) from *PO* consisting of arabinose and xylose, glucoxylan (*GX*) from *MP* consisting of glucose and xylose, and galactoarabinorhamnan (*GAR*) from *LR* consisting of galactose, arabinose, and rhamnose, where the last part of the name was due to the major monosaccharide content.

Table 1. Monosaccharide and elemental analysis of the hemicelluloses obtained from the plant materials.

Material	Monosaccharide content (% of total monosaccharides on anhydrous basis)						Elemental analysis (% anhydrous)			
	Ara	Gal	Glc	Xyl	Rh	GlcA	GalA	C	H	N
<i>PO</i>	23.40 \pm 0.13	ND	ND	76.91 \pm 0.46	ND	ND	ND	34.43 \pm 0.01	5.08 \pm 0.06	ND
<i>MP</i>	ND	ND	30.28 \pm 0.41	69.13 \pm 0.55	ND	1.02 \pm 0.15	ND	29.83 \pm 0.05	4.63 \pm 0.022	ND
<i>LR</i>	29.44 \pm 0.31	1.41 \pm 0.02	ND	ND	69.74 \pm 0.51	ND	1.82 \pm 0.24	41.98 \pm 0.04	6.08 \pm 0.01	ND

The data represent mean values ($n = 5$) \pm standard deviation.

Ara: Arabinose; Gal: Galactose; Glc: Glucose; Xyl: Xylose; Rh: Rhamnose; GlcA: Glucuronic acid; GalA: Galacturonic acid; ND: Not detected.

The FT-IR spectra (Fig. 1) exhibited typical bands of polysaccharides ($1200\text{--}800\text{ cm}^{-1}$) as reported for similar materials.^[30] A band centered around 1030 cm^{-1} was assigned to C–OH bending with shoulder peaks at $\sim 1159\text{ cm}^{-1}$, and the band at $\sim 895\text{ cm}^{-1}$ was due to antisymmetric C–O–C stretching of the glycosidic and β -1,4-linkages.^[31] The other characteristic bands were: $3419\text{--}3446\text{ cm}^{-1}$ (OH stretching), $2904\text{--}2923\text{ cm}^{-1}$ (aliphatic saturated C–H stretching), $2895\text{--}2813\text{ cm}^{-1}$ (carboxylic acid C=O, O–H and methylene C–H stretches), $1631\text{--}1640\text{ cm}^{-1}$ (deformation band of absorbed H_2O merged with carboxylic group of uronic acids), $1364, 1387\text{ cm}^{-1}$ (δCH), $1245\text{--}1260\text{ cm}^{-1}$ (δ -antisym bridged oxygen), $1000\text{--}1200\text{ cm}^{-1}$ (ring, $\nu\text{C-O C}$, $\nu\text{C-C}$, $\nu\text{C-O}$, $\delta\text{C-OH}$ strongly influenced by branching). Hemicelluloses usually contain some fractions of sugar acids, which usually impart a weakly anionic character to the macromolecule.^[32] The absorption bands around 1618 and 1430 cm^{-1} were typical of carboxylate groups of the uronic acid residues^[29] and the bands in the regions of $610\text{--}630\text{ cm}^{-1}$ and $520\text{--}530\text{ cm}^{-1}$ (polymer backbone) were also observed. The region $800\text{--}1200\text{ cm}^{-1}$ provides information about anomeric nature, glycosidic linkages, ring and alcoholic groups.

The weighted-average molar masses as determined by GPC were $3.6 \times 10^6\text{ Da}$ (*PO*), $2.5 \times 10^6\text{ Da}$ (*MP*), and $3.8 \times 10^6\text{ Da}$ (*LR*). These values are similar to those already reported.^[6]

MALDI-TOF mass spectrometry

MALDI-ToF mass spectra exhibited some important structural features of the water-soluble fractions of the hemicelluloses under investigation. GPC

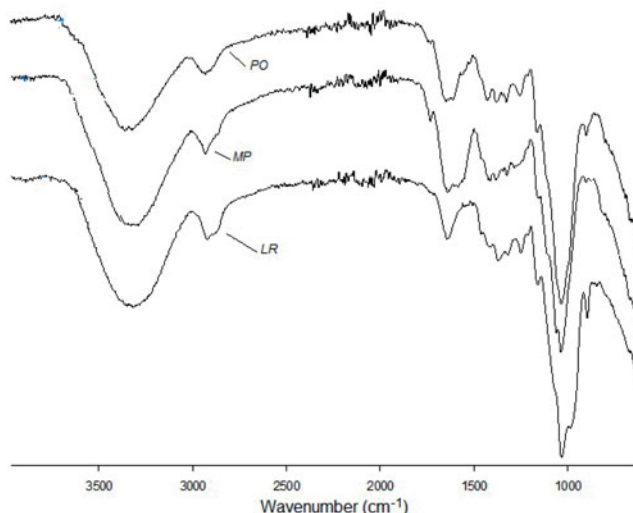


Figure 1. FT-IR spectra of hemicelluloses from *PO*, *MP*, and *LR*.

is a widely used technique for determination of the molar mass of polysaccharides, but sometimes there are resolution problems. Moreover, molar mass and hydrodynamic radius data generally do not correlate linearly.^[33,34] On the other hand, MALDI-ToF is considered to be more useful for determination of molar mass.^[35] Use of different matrices for the analysis of non-derivatized oligosaccharides by MALDI-ToF has been reported.^[16] 2,5-Dihydroxybenzoic acid (2,5-DHB) has been demonstrated to afford better reproducibility and higher signal-to-noise ratio.^[36] Therefore, this matrix was used in the present work. We were successful in detecting signals beyond 20,000 Da albeit at the relatively lower resolution and sensitivity. The spectra beyond 15,000 Da were disregarded due to very high noise and poor resolution. Most of the peaks observed were due to sodiated or protonated polysaccharide ions. The alkanization or protonation of fragment ions may give rise to several types of singly or doubly charged ions at particular m/z ratios like $[M + H]^+$, $[M + 2H]^{2+}$, $[M + Na]^+$, and $[M + H + Na]^{2+}$. The cationization mechanism of some polymers and peptides in MALDI has been investigated by different groups.^[21,36,37] These studies concluded that in case of polysaccharides, alkanization occurred more frequently than protonation. Most of the peaks observed were due to sodiated or protonated hemicellulose ions. The spectra of the hemicelluloses under investigation are discussed in detail in the following paragraphs.

Plantago Ovata

The spectra of hemicellulose from *PO* husk are shown in Figure 2. The striking features of the spectrum are: (i) A large number of signals between m/z 200–850 having good intensity suggested that low-mass fragments predominate. This may be due to fragmentation of highly-branched fractions occurring in the ionization chamber and/or polydispersity of water-soluble fractions of the polymer. (ii) Four signals around m/z 303, 435, 567, and 699, spaced by 132 Da (Fig. 2), suggest successive cleavages at the glycosidic bond. The signal at m/z 699.137 $[M + Na]^+$ represents an oligomer having five degrees of polymerization (DP). Such types of signals are categorized as Y-type according to Domon and Costello.^[38,39] (iii) A series of low-intensity signals due to $[M + H]^+$ (Y-type) were observed around m/z 266, 397, 529, and 661 spaced by 132 Da (Fig. 2). The protonation is possibly due to the presence of uronic acid residues as indicated by the FT-IR analysis. Here again, the highest m/z peak corresponds to DP = 5. The lower intensity is understandable as the carbohydrates are not easily protonated.^[40] Besides glycosidic cleavages, several lower intensity peaks (as compared with the peak at m/z 699) spaced by 60 Da (loss of $C_2H_4O_2$) and

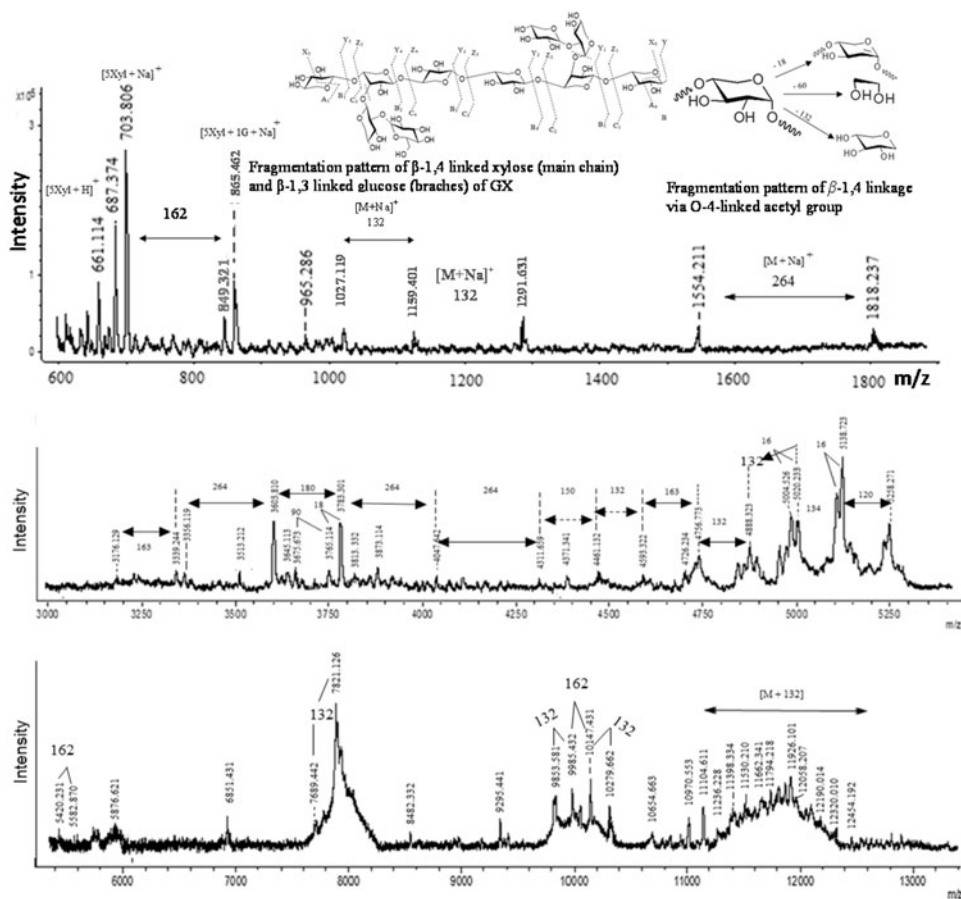


Figure 3. MALDI-ToF MS in the range m/z 600–13,000 and fragmentation patterns of GX. Nomenclature is according to Domon and Costello.^[38,39]

to 3750 differing by 18 Da representing the fragments after the loss of a water molecule. In addition to these, signals having a difference of 16 Da possibly due to Na^+/K^+ exchanges were also observed. Fragments smaller than m/z 200 were not detected in MALDI-ToF owing to the low-mass gate value used. It may be noted that pentosyl residues of Ara and Xyl can easily add to H^+ and Na^+ , which are isobaric. Therefore, the fragments cannot be correctly identified as originating from side chains or main chain and as such, the degree of polymerization from this data does not reflect the real monosaccharide content of the repeating unit.

Mimosa Pudica

The spectrum of the fraction from MP seeds is shown in Figure 3. Assignments of fragment ions were done by mass interval analysis. This

mucilage mainly consists of Xyl (69.11%) and Glc (30.89%) as recently reported.^[6] The mass of the singly charged xylosyl ion was calculated as: $(132) n + 23$ Da or $(132) n + 23 + 18$ Da (mass of reducing end residue) and that of glucosyl $(162) n + 23$ Da or $(162) n + 23 + 18$ Da and $(162) n + (132) n + 23$ Da, where n is the number of monosaccharide units. The masses 132 and 162 are due to Y/B fragmentation (glycosidic cleavage) and 18 Da is the mass of reducing end consisting of two H and one O, respectively.

Higher intensity peaks were observed in the range of m/z 600–900; the highest intensity peak at m/z 703 (expected 701) was identified as molecular ion peak and can be assigned to a $[5 \text{ Xyl} + \text{Na} + 18]^+$ adduct due to glycosidic cleavage of Xyl residues having the reducing end. The mass difference of daughter ion peaks corresponding to the parent ion was used to identify the glycoside position of the monosaccharide. The neighboring peaks of ions at m/z 643.374 and m/z 625.611 with a mass difference of 60 and 78 Da are due to loss of $\text{C}_2\text{H}_4\text{O}_2$ (cross-ring; A/X-type) and $\text{C}_2\text{H}_4\text{O}_2 + 18$, respectively. This suggests the cleavage of β -1,4-linked xylosyl residue and reducing end (60 + 18), respectively, which corresponds to a loss of xylosyl residues in the polysaccharide backbone. This was further supported by the absence of any high-intensity peak around m/z 673 (with a mass difference of 30 Da). A peak at m/z \sim 865 with a mass difference of 162 Da represents the presence of a hexosyl residue $[\text{Xyl-Xyl-Xyl-Xyl-Xyl-Glc} + \text{Na}]^+$. Two peaks of low intensity were observed with mass differences of 16 and 120 Da at m/z \sim 849 and m/z \sim 745, respectively. These differences suggest that Glc is also linked to Xyl through β -1,4-linkage. The intensities of these signals suggest that these are present as branches on the main chain. This is because bulky groups are more vulnerable to fragmentation.

The low-intensity peak at m/z \sim 661 may be due to dehydrated monoprotonated five xylosyl residues $[\text{Xyl-Xyl-Xyl-Xyl-Xyl} + \text{H} - \text{H}_2\text{O}]^+$ at the glycosidic position. The lower intensity signal of the fragment is understandable as discussed above. Very low-intensity peaks were observed in the m/z range of 900–3500. A careful observation indicates that these peaks consist of two weak signals spaced by 162 Da (due to loss of Glc) at m/z 865 and 1027. The m/z 1027 represents the sequence $[\text{Xyl-Xyl-Xyl-Xyl-Xyl-Glc-Glc} + \text{Na} + 18]$. Peaks at m/z 1159 and 1291 spaced by 132 Da were due to loss of Xyl. Two peaks at m/z 1554.211 and 1818.237 (Fig. 3a) correspond to the loss of Xyl-Xyl, but the dimer formation at the laser frequency used in these experiments appears to be not a good assumption. Thus, this series of peaks is assigned to sodiated or protonated fragments of Y_i/B_i -type. These spectra exhibited signals corresponding to A/X-type cross-ring fragmentation, therefore, it can be concluded that xylosyl and

glucosyl residues are also linked through β -1,3-linkage somewhere along with β -1,4 positions. The lower intensities of these peaks indicate that this material consists of a rigid linear chain difficult to undergo fragmentation. Some signals of middle intensity were observed in the m/z range 3400–12,500 with significant mass differences. In this region, bunches of peaks having a very low resolution, due to use of reflectron mode, were observed from m/z 8000–13,000 with the highest molecular ion peak around m/z 12,000. A careful speculation is that the bunch consists of a regular series of signals with mass differences of ~ 132 and 162 Da corresponding to xylosyl or glucosyl residues $[M + Na]^+$ or $[M + H]^+$. This was the highest mass ever detected by MALDI-ToF in polysaccharides, which corresponds to about 90 monosaccharides units of Xyl (Fig. 3). The above assignments of the high m/z peaks may not be valid because of lower resolution and sensitivity in these spectra; usually, the polysaccharide length of 40–45 is observable.

Several signals with differences of 16 Da possibly due to Na^+/K^+ exchanges were also observed. The spectrum exhibited some signals with a mass difference of 192 Da ($60 + 132$) confirming the presence of uronic acid residues in this material including the reducing ends. Such peaks were observed at m/z 2306.316, 2366.714, and 2499.366 (Fig. 3). The peaks with m/z difference of ~ 162 in the mass range 600–900 Da are due to glycosidic cleavages of hexose units. As this material has been reported to contain Xyl and Glc monomers, the difference of 162 Da can be considered due to glucosyl, which is cleaved by Y/B or Z/C type fragmentation. The main chain of *MP* appears to consist of β -1,4-d-xylose molecules with Glc molecules linked through β -1,3-linkage either in the main chain or in the branches. Based on this evidence, a structure of *MP* hemicellulose can be proposed as shown in (Fig. 3). Thus, the material can be named as GX.

Lallemantia Royleana

The spectrum of the fraction from *LR* seeds is shown in Figure 4. This material consists of Gal (1.28%), Ara (29.14%), and Rh (69.59%) as reported previously.^[6] The key fragments obtained in the spectra corresponded to specific structural elements of hemicelluloses. A large number of peaks of varying intensity were observed in low to high mass range, suggesting an intensive branching and diverse heterogeneity of the hemicellulose. In low-mass region, the highest intensity peak was at m/z 917.168; this was assigned to a sodiated-ion of six Rh units as a result of glycosidic cleavage from the reducing end (Y/B type fragmentation). The 146 Da mass represents Rh after glycosidic cleavage. The mass difference of daughter fragments of m/z 917.168 peak was helpful in determining the linking pattern of the

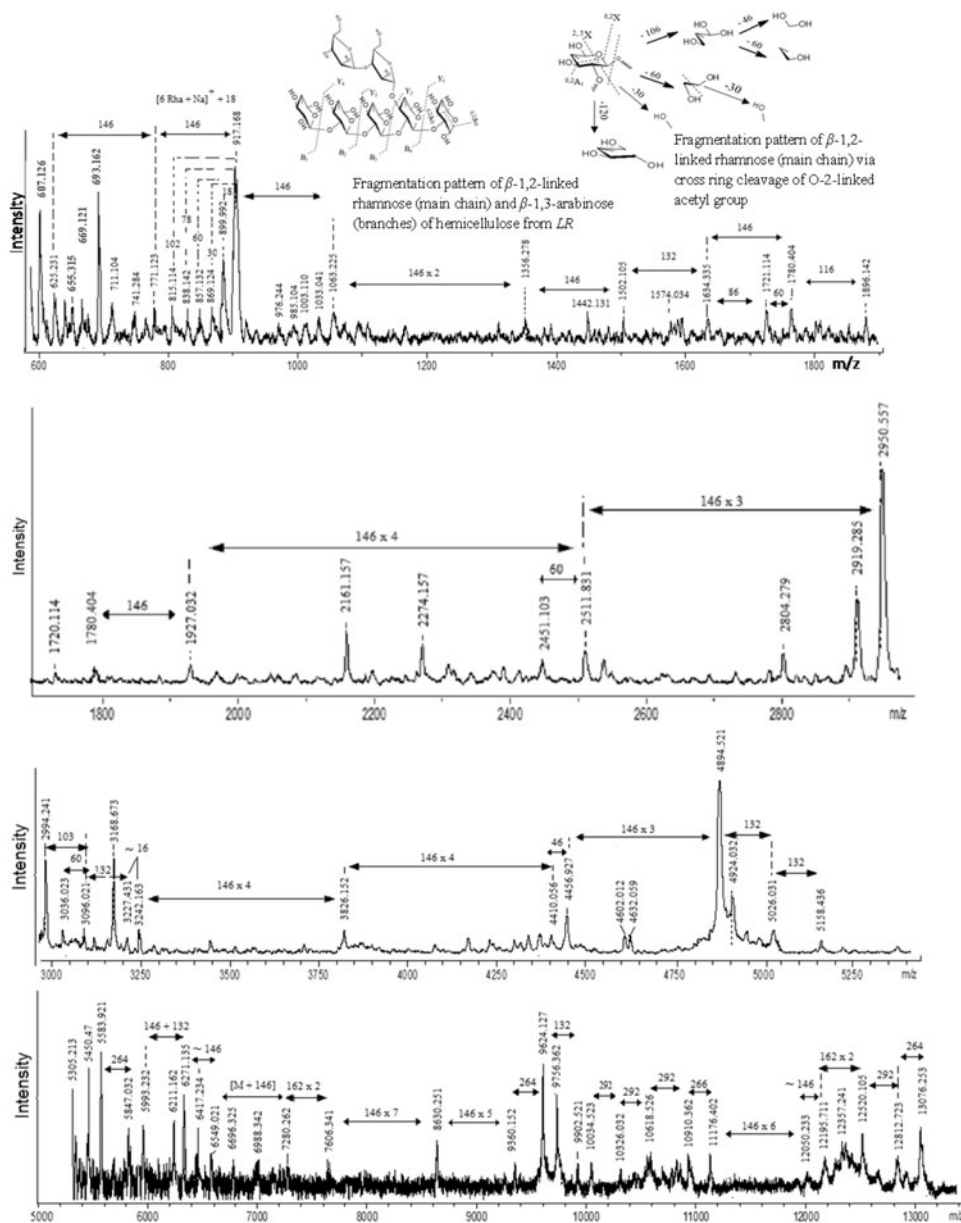


Figure 4. MALDI-TOF MS in range m/z 600–13,000 and fragmentation of GAR. Nomenclature is according to Domon and Costello.^[38,39]

monosaccharides. A neighboring peak at m/z 899 with mass difference of 18 Da corresponds to a loss of reducing end (Z-type fragmentation). Other peaks at m/z 869, 857, and 815 were observed with a mass difference of 30, 60, 78, and 102 Da, which are characteristic of β -1,2-linkage of monosaccharides including the acetyl group. A signal of relatively lower intensity was observed at m/z 771, which corresponds to the sodiated peak of five Rh residues (Y-type fragmentation). The peak at m/z 693 having a mass difference

of 78 indicates a β -1,2-linkage in this material. The neighboring peaks at m/z 603, 633, 663, and 675 with mass differences of 90, 60, 30, and 18 Da also suggests β -1,2-linkages of monosaccharides. A noticeable feature in the spectrum was that the cross-ring fragmentation produced higher intensity peaks as compared to those due to glycosidic cleavages.

There was no peak having a considerable intensity between m/z 920 and 2000. However, a few peaks of very low intensity were observed at regular intervals with mass difference of 146 Da or multiple of it at m/z 1063 ($[7\text{ Rh} + \text{Na} + 18]^+$), 1356, and 1502 indicating the presence of fragments representing $[M + 146 + \text{Na}]^+$. Two low-intensity signals at m/z 1502 and 1634 (mass difference of 132 Da) were observed, which corresponds to a pentosyl residue after glycosidic cleavage that is Ara in this case. The lower intensity reflects that Ara may be a part of the main chain. Beyond m/z 2100–13,000, there were a number of high-intensity signals. Interestingly, the mass difference between various peaks represented the di-, tri-, and tetra-mers of Rh (Fig. 4). These assignments may be considered with caution because of lower resolution and sensitivity in these spectra. The high-intensity signals suggest that fragments are generated from side chains. A bunch of peaks was present in the higher mass range beyond m/z 12,000 as observed in the spectrum of *MP*. The mass difference of 162 Da between the closely spaced peaks in the bunch suggests the presence of hexosyl (Gal) residues in the hemicellulose. Presence of several high-intensity signals reveals that hemicellulose is highly branched. The spectrum was dominated by peaks resulting from cleavage at glycosidic bonds, giving the Y/C-type ion series and a less intense series of Z/B-type ions. Moreover, the regular appearance of blocks of Rh having at least one reducing end suggests that the fragmentation at reducing end was more common than at non-reducing end. These results suggest that Ara and Rh are a part of the main chain, whereas other monosaccharides are most probably from branches. Some signals with a mass difference of 176 and 192 were detected between m/z 3000 and 3250, which confirms the presence of uronic acids. These results are also in line with those of an NMR study^[43], which authenticates the potential of MALDI-ToF mass spectrometry in structure elucidation of hemicelluloses.

Materials and methods

Materials

PO seeds husk, *MP*, and *LR* seeds (all purchased from herbal product shops in local market). L(+)-arabinose, D(+)-galactose, D(+)-glucose, D(+)-xylose, L(\pm)-rhamnose monohydrate, D(+)-glucuronic acid, D(+)-galacturonic acid, and 2,5-dihydroxybenzoic acid (DHB), all from Sigma-Aldrich, USA. Citric

acid, disodium hydrogen phosphate, and hydrochloric acid were from E. Merck, Germany, and lactose from Sheffield Bio-Science, UK. Oligosaccharides β -(1-4)-D-xylotriase, β -(1-4)-D-xylotetraose, β -(1-4)-D-xylopentaose, and β -(1-4)-D-xylohexaose used as GPC standards were from Megazyme (Sydney, Australia). All the chemicals were used without further purification. Distilled water was used throughout this study.

Isolation of mucilage of PO seed husk, MP and LR seeds

Seed husk of *PO*, *MP*, and *LR* seeds (1.0 g) were de-dusted by sifting and soaked in water (500 mL) for 24 h. It was homogenized by the use of kitchen blender and translucent material was isolated by vacuum filtration through a muslin cloth. The mucilage was freed from fibers by centrifugation at 3000 rpm for 15 min. To this, water (\sim 100 mL) was added and the suspension was centrifuged again. This process was repeated two more times to get clean mucilage. A clear translucent gel-like material thus obtained was concentrated by vacuum evaporation, desalted, and freeze-dried. The powder was stored in a desiccator till its use for analysis.

Elemental analysis

Elemental analysis of materials was performed on CHNS analyzer Vario MICRO V1.4.2 (Elementar Analysen Systeme, GmbH, Germany).

Monosaccharide analysis

Monosaccharide analysis was performed after acid hydrolysis of the sample^[44] by using Dionex ICS 3000 HPLC system, consisting of: CarboPacPA20 column (0.4×150 mm) and electrochemical detector, according to a reported method.^[45] The chromatographic conditions were: isocratic elution using 95% water and 5% 0.2 M NaOH at room temperature (25 ± 1 °C); flow rate 0.5 mL min^{-1} ; injection volume $50 \mu\text{L}$.

FTIR analysis

FTIR spectra were recorded in a transmission mode by using thin films of the samples, obtained by drying 0.5 mL of aqueous suspension (5 mg mL^{-1}) at ~ 40 °C for 4 h, using IR-prestige-20 spectrophotometer (Shimadzu, Japan).

Gel permeation chromatography

GPC was carried out on PL Aquagel-OH mixed column (8 μm ; 7.5 \times 300 mm), a macroporous copolymer bead with an extremely hydrophilic polyhydroxyl functionality, from Agilent 1200 series (Agilent, Germany) equipped with Quat pump (G1311A) and refractive index detector (G1362A) using water containing 0.1% NaNO_3 as eluent (flow rate: 1.0 mL min^{-1} at 70 $^\circ\text{C}$) and injection volume of 10 μL . The sample (0.1% w/v) was filtered through 0.45 μm membrane filter before injection. Data were analyzed by the use of Chem-Station GPC Data Analysis Rev. A.02.02 (Agilent, Germany).

MALDI-ToF mass spectrometry

MALDI-ToF mass spectra of the samples were recorded by Bruker Ultraflex extreme MALDI-ToF/ToF (Bruker Daltonics Inc, USA) spectrometer using single ToF option. The desalted sample (1.5 μL) was spotted in triplicate on MTP 384 polished steel BC targets (Bruker Daltonics). Samples were overlaid with 2,5-DHB (1.5 μL) and left for drying (dried droplet method). Matrix solubilization procedure included dissolution of 2,5-DHB (20 mg mL^{-1}) in acetonitrile-0.1% TFA in water (30:70 v/v) supplemented with 1 mM NaCl . Spectra were recorded from m/z 200 to 25,000 Da in reflectron mode. The instrument settings were: pulsed ion extraction 70 ns, laser frequency 1000 Hz, and a number of shots per sample 10,000. The spectra beyond 15,000 Da were very noisy, so they were excluded.

Conclusions

The MALDI-ToF MS analysis successfully elucidated the structural features in the hemicelluloses under investigation. The study identified the presence of β -1,4-linked xylose with arabinose attached to main chain at β -1,3 positions (*Plantago ovata*), β -1,4-linked xylose with glucose attached to main chain at β -1,3 positions (*Mimosa pudica*), and β -1,2-linked rhamnose and β -1,3-linked arabinose units in the main chain with arabinose attached to the main chain through β -1,3-linkage (*Lallemantia royleana*). These results are in line with those from NMR studies reported previously. This study demonstrated that use of 2,5-DHB as the matrix can yield quite informative mass spectra from non-derivatized water-soluble fractions of the hemicelluloses. However, the overall detection efficiency compared to that for proteins was low; this necessitates a search for a still better matrix for the structural study of hemicelluloses. The challenge is posed by a high degree of heterogeneity associated with the hemicelluloses, which produce complex mass spectra.

Acknowledgement

The authors thank Institute of Cancer and Genomic Sciences, University of Birmingham, UK, for MALDI-ToF analysis and Dr. Bettina Wolf, Division of Food Sciences, School of Biosciences, University of Nottingham, Sutton Bonington Campus, Loughborough and Dr. David Coles, School of Biosciences, University of Nottingham, UK, for assistance in mono-saccharide analysis.

Funding

FI acknowledges HEC Pakistan under IRSIP for a grant for working at University of Birmingham, UK. SM and MSI acknowledge a research grant from HEC Pakistan [No. 20-3775/NRPU/R&D/HEC/14/1220].

ORCID

Fozia Iram  <http://orcid.org/0000-0001-7252-2164>

Mohammad S Iqbal  <http://orcid.org/0000-0002-2933-195X>

Douglas G. Ward  <http://orcid.org/0000-0002-2328-1445>

References

- [1] Gencturk, A.; Kahraman, E.; Güngör, S.; Özhan, G.; Özsoy, Y.; Sarac, A.S. Polyurethane/hydroxypropyl cellulose electrospun nanofiber mats as potential transdermal drug delivery system: characterization studies and in vitro assays. *Artif. cells Nanomed. Biotechnol.* **2016**, *1401*, 1–10.
- [2] Aytac, Z.; Sen, H.S.; Durgun, E.; Uyar, T. Sulfisoxazole/cyclodextrin inclusion complex incorporated in electrospun hydroxypropyl cellulose nanofibers as drug delivery system. *Colloids Surf. B Biointerfaces.* **2015**, *128*, 331–338.
- [3] Barkhordari, S.; Yadollahi, M.; Namazi, H. pH sensitive nanocomposite hydrogel beads based on carboxymethyl cellulose/layered double hydroxide as drug delivery systems. *J. Polym. Res.* **2014**, *21*, 454.
- [4] Buhus, G.; Popa, M.; Desbrieres, J. Hydrogels based on carboxymethylcellulose and gelatin for inclusion and release of chloramphenicol. *J. Bioact. Compat. Pol.* **2009**, *24*, 525–545.
- [5] Omidian, H.; Park, K. Swelling agents and devices in oral drug delivery. *J. Drug Deliv. Sci. Technol.* **2008**, *18*, 83–93.
- [6] Massey, S.; Iqbal, M.S.; Wolf, B.; Mariam, I.; Rao, S. Comparative drug loading and release study on some carbohydrate polymers. *Lat. Am. J. Pharm.* **2016**, *35*, 146–155. http://www.latamjpharm.org/resumenes/35/1/LAJOP_35_1_1_22.pdf
- [7] Akbar, J.; Iqbal, M.S.; Massey, S.; Masih, R. Kinetics and mechanism of thermal degradation of pentose- and hexose-based carbohydrate polymers. *Carbohydr. Polym.* **2012**, *90*, 1386–1393.
- [8] Iqbal, M.S.; Akbar, J.; Saghir, S.; Karim, A.; Koschella, A.; Heinze, T.; Sher, M. Thermal studies of plant carbohydrate polymer hydrogels. *Carbohydr. Polym.* **2011**, *86*, 1775–1783.

- [9] Nasri-Nasrabadi, B.; Mehrasa, M.; Rafienia, M.; Bonakdar, S.; Behzad, T.; Gavanji, S. Porous starch/cellulose nanofibers composite prepared by salt leaching technique for tissue engineering. *Carbohydr. Polym.* **2014**, *108*, 232–238.
- [10] Tampieri, A.; Sprio, S.; Ruffini, A.; Celotti, G.; Lesci, I.G.; Roveri, N.; Semmelmann, K.; Carlos, A.D.; Varela-Feria, F.M.; Martinez-Fernandez, J.; Arellano-Lopez, A.R.D. From wood to bone: multi-step process to convert wood hierarchical structures into biomimetic hydroxyapatite scaffolds for bone tissue engineering. *J. Mater. Sci. Mater. Med.* **2000**, *11*, 743–749.
- [11] Teeri, T.T.; Brumer, H.; Daniel, G.; Gatenholm, P. Biomimetic engineering of cellulose-based materials. *Trends Biotechnol.* **2007**, *25*, 299–306.
- [12] Johnson, L.M.; Li, Z.; LaBelle, A.J.; Bates, F.S.; Lodge, T.P.; Hillmyer, M.A. Impact of polymer excipient molar mass and end groups on hydrophobic drug solubility enhancement. *Macromolecules* **2017**, *50*, 1102–1112.
- [13] Baldwin, A.D.; Kiick, K.L. Polysaccharide-modified synthetic polymeric biomaterials. *Biopolymers* **2010**, *94*, 128–140.
- [14] Kim, C.J. Effects of drug solubility, drug loading, and polymer molecular weight on drug release from Polyox[®] tablets. *Drug. Dev. Ind. Pharm.* **1998**, *24*, 645–651.
- [15] Broberg, S.; Broberg, A.; Duus, J.O. Matrix-assisted laser desorption/ionization time-of-flight. *Rapid Commun. Mass Spectrom.* **2000**, *14*, 1801–1805.
- [16] López-García, M.; García, M.S.D.; Vilarino, J.M.L.; Rodríguez, M.V.G. MALDI-TOF to compare polysaccharide profiles from commercial health supplements of different mushroom species. *Food Chem.* **2016**, *199*, 597–604.
- [17] Hao, C.; Ma, X.; Fang, S.; Liu, Z.; Liu, S.; Song, F.; Liu, J. Positive- and negative-ion matrix-assisted laser desorption/ionization mass spectrometry of saccharides. *Rapid Commun. Mass Spectrom.* **1998**, *12*, 345–348.
- [18] Iqbal, M.S.; Massey, S.; Akbar, J.; Ashraf, C.M.; Masih, R. Thermal analysis of some natural polysaccharide materials by isoconversional method. *Food Chem.* **2013**, *140*, 178–182.
- [19] Iqbal, M.S.; Akbar, J.; Hussain, M.A.; Saghri, S.; Sher, M. Evaluation of hot-water extracted arabinoxylans from ispaghula seeds as drug carriers. *Carbohydr. Polym.* **2011**, *83*, 1218–1225.
- [20] Montaudo, G.; Montaudo, M.S.; Puglisi, C.; Samperi, F. Characterization of polymers by matrix-assisted laser desorption ionization-time of flight mass spectrometry. End group determination and molecular weight estimates in poly(ethylene glycols). *Macromolecules.* **1995**, *28*, 4562–4569.
- [21] Hung, W.T.; Wang, S.-H.; Chen, Y.-T.; Yu, H.-M.; Chen, C.-H.; Yang, W.-B. MALDI-TOF MS analysis of native and permethylated or benzimidazole-derivatized polysaccharides. *Molecules.* **2012**, *17*, 4950–4961.
- [22] Rohmer, M.; Meyer, B.; Mank, M.; Stahl, B.; Bahr, U.; Karas, M. 3-Aminoquinoline acting as matrix and derivatizing agent for MALDI MS analysis of oligosaccharides. *Anal. Chem.* **2010**, *82*, 3719–3726.
- [23] Ranasinghe, C.; Akhurst, R.J. Matrix assisted laser desorption ionisation time of flight mass spectrometry (MALDI-TOF MS) for detecting novel Bt toxins. *J. Invertebr. Pathol.* **2002**, *79*, 51–58.
- [24] Tang, W.; Nelson, C.M.; Zhu, L.; Smith, L.M. Positive ion formation in the ultraviolet matrix-assisted laser desorption/ionization analysis of oligonucleotides by using 2,5-dihydroxybenzoic acid. *J. Am. Soc. Mass Spectrom.* **1997**, *8*, 218–224.
- [25] Mock, K.K.; Davey, M.; Cottrell, J.S. The analysis of underivatized oligosaccharides by matrix-assisted laser desorption mass spectrometry. *Biochem. Biophys. Res. Commun.* **1991**, *177*, 644–651.

- [26] Stahl, B.; Steup, M.; Karas, M.; Hillenkamp, F. Analysis of neutral oligosaccharides by matrix-assisted laser desorption ionization mass spectrometry. *Anal. Chem.* **1991**, *63*, 1463–1466.
- [27] Matamoros Fenández, L.E.; Sørensen, H.R.; Jørgensen, C.; Pedersen, S.; Meyer, A.S.; Roepstorff, P. Characterization of oligosaccharides from industrial fermentation residues by matrix-assisted laser desorption/ionization, electrospray mass spectrometry, and gas chromatography mass spectrometry. *Mol. Biotechnol.* **2007**, *35*, 149–160.
- [28] Sakai, S.; Hirano, K.; Toyoda, H.; Linhardt, R.J.; Toida, T. Matrix-assisted laser desorption ionization-time of flight mass spectrometry analysis of hyaluronan oligosaccharides. *Analyt. Chim. Acta.* **2007**, *593*, 207–213.
- [29] Laidlaw, R.A.; Percival, E.G.V. 101. Studies of seed mucilages. Part V. Examination of a polysaccharide extracted from the seeds of *Plantago Ovata* forsk by hot water. *J. Chem. Soc.* **1950**, 528–534.
- [30] Saghir, S.; Iqbal, M.S.; Hussain, M.A.; Koschella, A.; Heinze, T. Structure characterization and carboxymethylation of arabinoxylan isolated from ispaghula (*Plantago Ovata*) seed husk. *Carbohydr. Polym.* **2008**, *74*, 309–317.
- [31] Barron, C.; Rouau, X. FTIR and Raman signatures of wheat grain peripheral tissues. *Cereal Chem.* **2008**, *85*, 619–625.
- [32] Wang, Q.; Ellis, P.R.; Ross-Murphy, S.B. Dissolution kinetics of Guar gum powders—III. Effect of particle size. *Carbohydr. Polym.* **2006**, *64*, 239–246.
- [33] Kaushik, A.; Tiwari, A.; Gaur, A. Role of excipients and polymeric advancements in preparation of floating drug delivery systems. *Int. J. Pharma. Investig.* **2015**, *5*, 1.
- [35] Nep, E.I.; Conway, B.R. Physicochemical characterization of Grewia polysaccharide gum: Effect of drying method. *Carbohydr. Polym.* **2011**, *84*, 446–453.
- [35] Hsu, N.Y.; Yang, W.-B.; Wong, C.H.; Lee, Y.-C.; Lee, R.T.; Wang, Y.S.; Chen, C.-H. Matrix-assisted laser desorption/ionization. *Rapid Commun. Mass Spectrom.* **2007**, *21*, 2137–2146.
- [36] Liao, P.-C.; Allison, J. Ionization processes in matrix-assisted laser desorption/ionization mass spectrometry: matrix-dependent formation of $[M + H]^+$ Vs $[M + Na]^+$ ions of small peptides and some mechanistic comments. *J. Mass Spectrom.* **1995**, *30*, 408–423.
- [37] Wang, Y.; Rashidzadeh, H.; Guo, B. Structural effects on polyether cationization by alkali metal ions in matrix-assisted laser desorption/ionization. *J. Am. Soc. Mass Spectrom.* **2000**, *11*, 639–643.
- [38] Domon, B.; Costello, C.E. A systematic nomenclature for carbohydrate fragmentations in FAB-MS/MS spectra of glycoconjugates. *Glycoconjugate J.* **1988**, *5*, 397–409.
- [39] Viseux, N.D.; Hoffmann, E.; Domon, B. Structural assignment of permethylated oligosaccharide subunits using sequential tandem mass spectrometry. *Anal. Chem.* **1998**, *70*, 4951–4959.
- [40] Garozzo, D.; Giuffrida, M.; Impallomeni, G.; Ballistreri, A.; Montaudo, G. Determination of linkage position and identification of the reducing end in linear oligosaccharides by negative ion fast atom bombardment mass spectrometry. *Anal. Chem.* **1990**, *62*, 279–286.
- [41] Yu, L.; Yakubov, G.E.; Zeng, W.; Xing, X.; Stenson, J.; Bulone, V.; Stokes, J.R. Multi-layer mucilage of *Plantago Ovata* seeds: Rheological differences arise from variations in arabinoxylan side chains. *Carbohydr. Polym.* **2017**, *165*, 132–141.
- [42] Fischer, M.H.; Yu, N.; Gray, G.R.; Ralph, J.; Anderson, L.; Marlett, J.A. The gel-forming polysaccharide of Psyllium husk (*Plantago Ovata* Forsk). *Carbohydr. Res.* **2004**, *339*, 2009–2017.

- [43] Farhadi, N. Structural elucidation of a water-soluble polysaccharide isolated from Balangu Shirazi (*Lallemantia Royleana*) seeds. *Food Hydrocoll.* **2017**, *72*, 263–270.
- [44] Saeman, J.F.; Moore, W.E.; Mitchell, R.L.; Millett, M.A. Techniques for the determination of pulp constituents by quantitative paper chromatography. *Tappi J.* **1954**, *37*, 336–343.
- [45] Weitzhandler, M.; Barreto, V.; Pohl, C.; Jandik, P.; Cheng, J.; Avdalovic, N. CarboPacTM PA20: A new monosaccharide separator column with electrochemical detection with disposable gold electrodes. *J. Biochem. Biophys. Methods.* **2004**, *60*, 309–317.